Figure S1. Gene targeting strategies.

Wild-type gene structures, targeting vectors, and correctly targeted alleles for H3f3a and H3f3b are shown. N: neomycin/G418 resistance gene open reading frame. E: EGFP. tdT: tdTomato. DTA: human EF1a promoter-driven diphtheria toxin expression cassette for negative selection. Primer locations for PCR screens and probe locations for Southern blot reconfirmation are labeled. A ~1kb insertion of repetitive sequence was present in the targeting vector but screened out in correctly targeted clones.

Figure S2. PCR screen gel and Southern blots showing identification of correctly targeted ES cell clones.

PCR and Southern blot results in targeted ES cell clone identification, corresponding to the strategies outlined in Figure S1. Red numbered clones were eventually used for blastocyst injection/chimera generation. The predicted sizes of products for untargeted wild-type (WT) and targeted (mut) alleles are labeled. Red-boxed areas in some Southern blot images were differentially adjusted to reduce signal intensity for sharper views of the relatively much stronger control signals.

Figure S3. RNA-seq samples and results.

(A) Gloss morphology of E10.5 embryos used in the RNA-seq experiment. Genotypes: Control: *H3f3a*$^{fl/+}$*; H3f3b*$^{fl/+}$*; Sox2-Cre*$^{Tg/0}$*; Trp53*$^{-/-}$, KO: *H3f3a*$^{fl/-}$*; H3f3b*$^{fl/-}$*; Sox2-Cre*$^{Tg/0}$*; Trp53*$^{-/-}$ (B) UCSC RNA-seq tracks at *H3f3a* and *H3f3b* loci. Red boxes highlight the floxed exons, whose expression was completely lost in the KO embryos. (C) MDS plot of the RNA-seq results. (D) Stacked column chart representation of data points in Fig. 6A. Illustrating distribution of genes of the total and changed population on their expression level range. (E) Stacked column chart representation of red data points in Fig. 6A,

illustrating the distribution of genes of different change levels on their expression level range. (F) RT-qPCR validation of six genes that showed no significant change in the RNA-seq results. (G) Total RNA yields from control and KO embryos. (H) UCSC Genome Graphs show distribution of significantly changed genes. Red and green bars indicate the genomic locations of up- and down-regulated genes, respectively. (H) MDS plot of RE expression in each embryo. (J) The edgeR smear plot visualization of REs identified in the RNA-seq results. The single RE with a significant change (FDR < 0.05) is plotted red.

Figure S4. IPA results on canonic pathways.

Figure S5. IPA results on disease and bio-function pathways.

Figure S6. ATRX binding to telomeres in H3.3 KO/*p53*^{null} MEFs.

ChIP-qPCR results were normalized to their respective inputs. Rabbit IgG is used as the control. SEM is from two biological replicates. No statistical difference was found.

Figure S7. Global levels of histone marks in MEFs, and FAIRE yields.

(A) and (E) Global level of different histone marks in H3.3 KO/*p53*^{null} and control MEFs, by western blot. Lane 2 and 4 are mutant cell lines; lane 1 and 3 are their littermate control lines, respectively. (B) and (F) Levels of respective signal strengths of (A) and (E) normalized to total H3 (for histone marks and CENP-A) or β-actin (for TRF proteins) levels. (C) Total yield of FAIRE-isolated DNA as percentage of input, two H3.3 KO MEF lines and their respective sibling control lines were used. (D) Verification of CENP-A and TRF1 antibody specificity. ChIP-qPCR results with respective antibodies and primers amplifying different repeat sequences and two non-repetitive intergenic sequences (Myc U3/U4, upstream of Myc gene promoter) as additional negative loci

control. Rabbit IgG serves as non-specific antibody control. Myc U4 locus enrichment level is set as one for normalization in both graphs. Two sibling MEF lines are used (N = 2).

Table S1. List of genes identified in RNA-seq data and statistical analysis results.

Table S2. List of genes identified in RNA-seq data and their annotated information.

Table S3. List of repetitive sequences identified in RNA-seq data and statistical analysis results.

Table S4. IPA results on canonic pathways.

Table S5. IPA results on disease and bio-function pathways.

Table S6. Primer sets used in gene expression and ChIP assays.

Table S7. Primer sets for genotyping.

Jang264150_Fig. S1

H3f3a

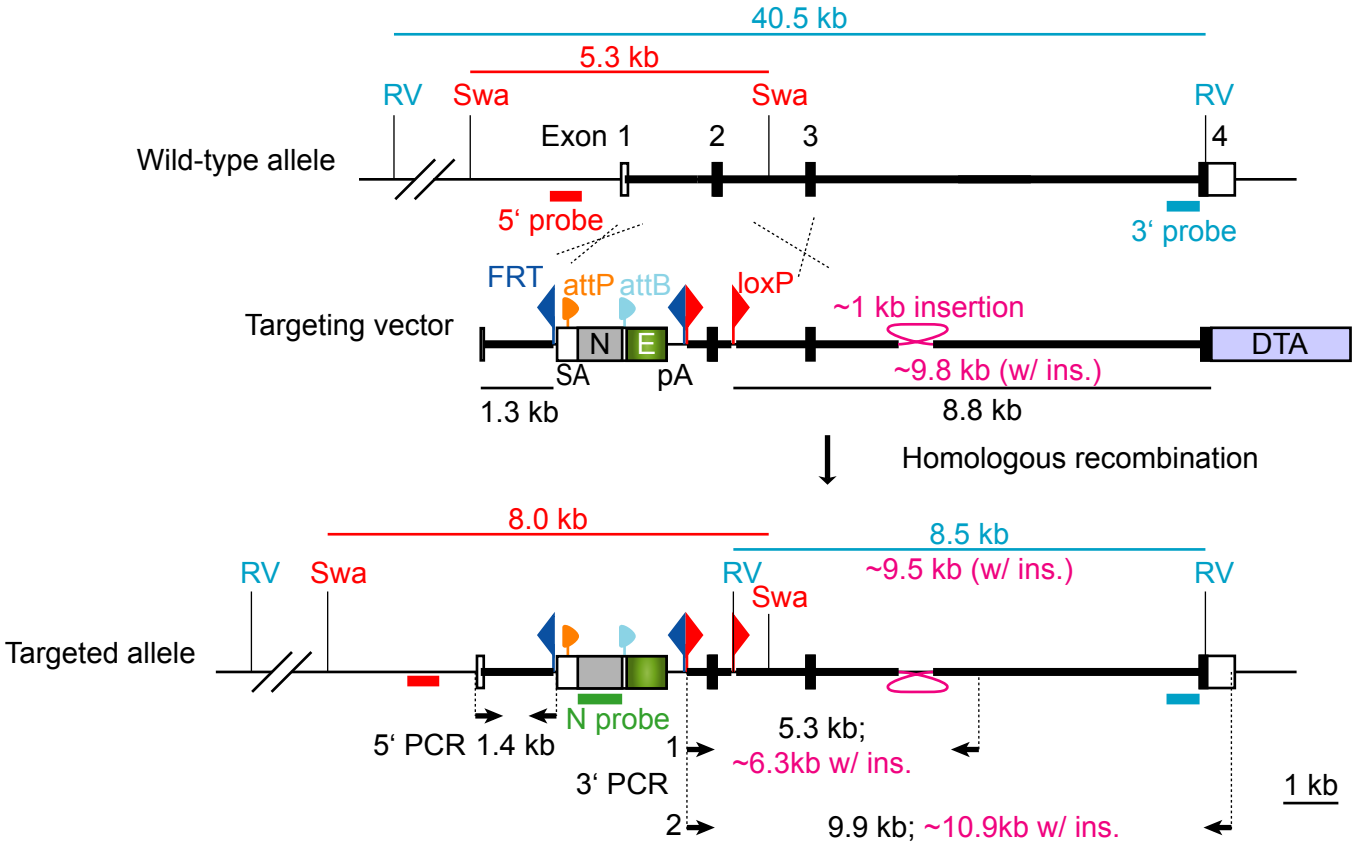

H3f3b

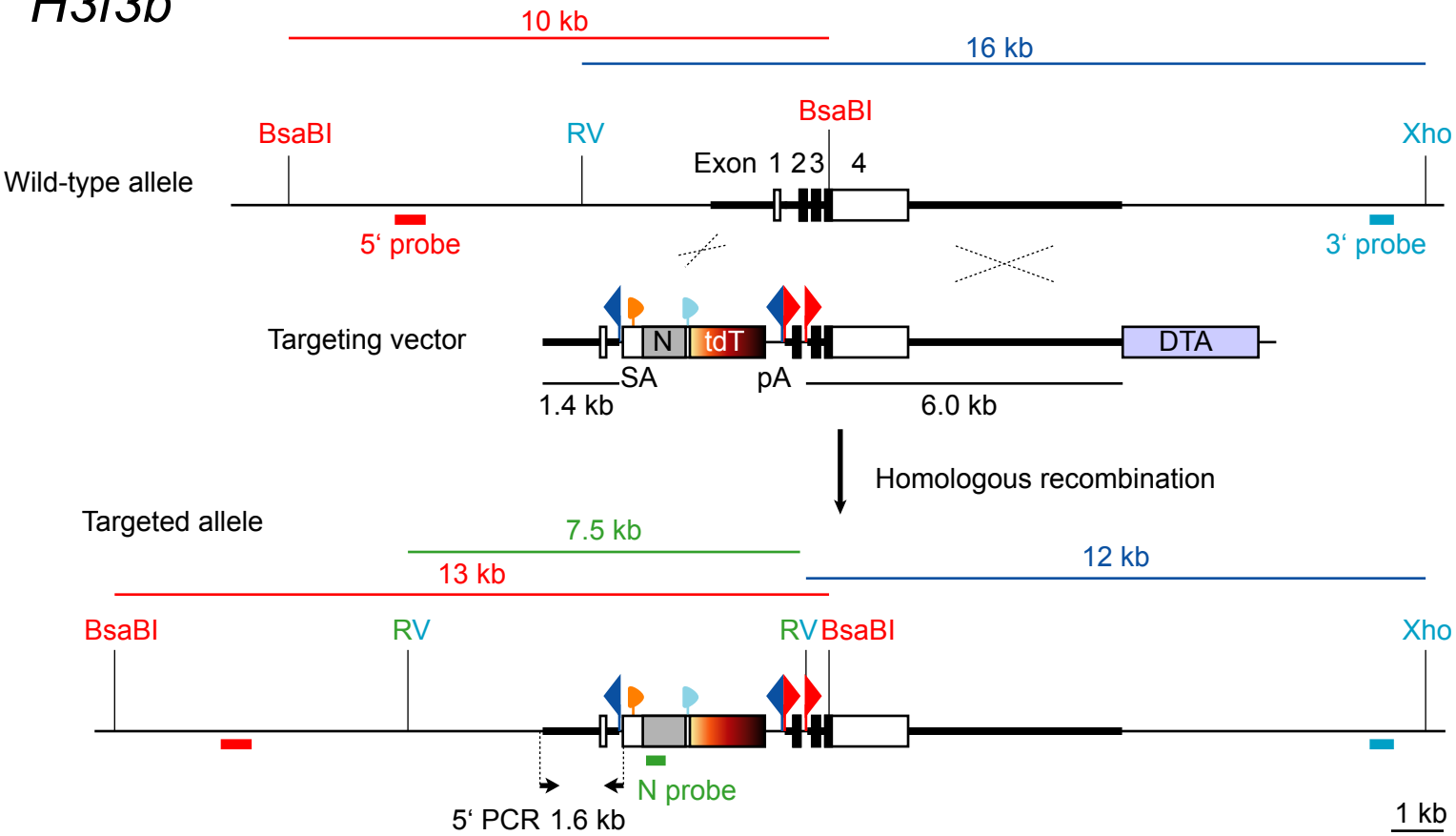

Jang264150_Fig. S2

H3f3a Targeting

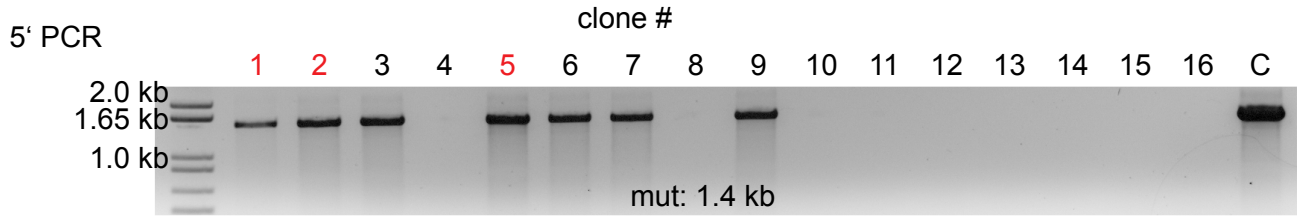

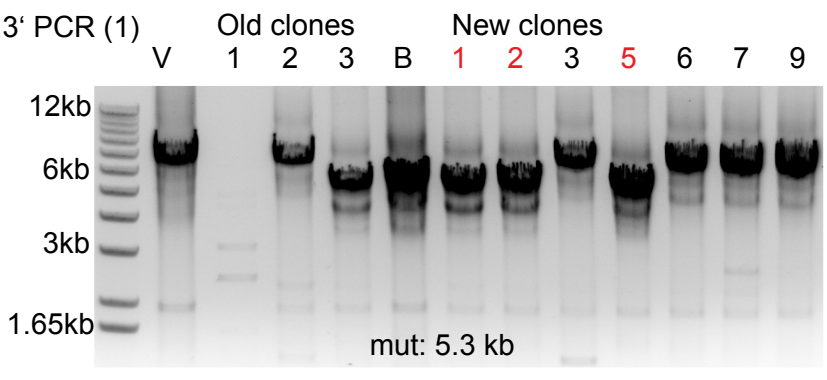

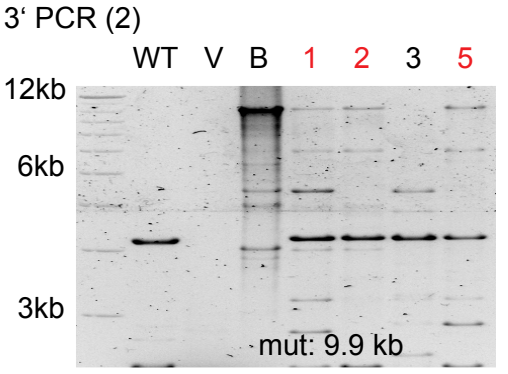

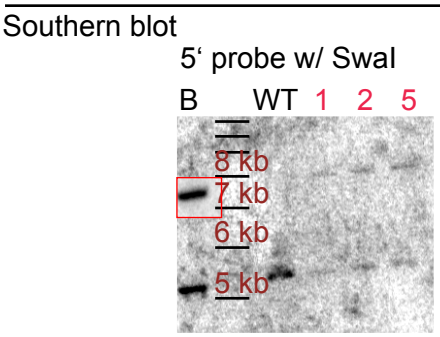

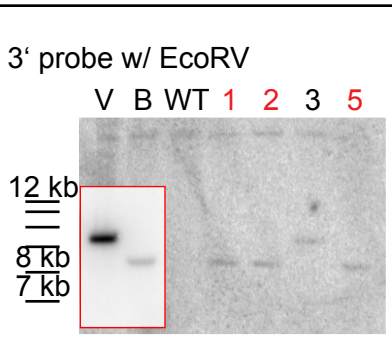

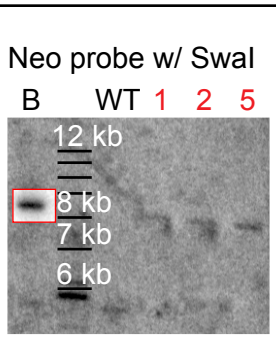

H3f3b Targeting

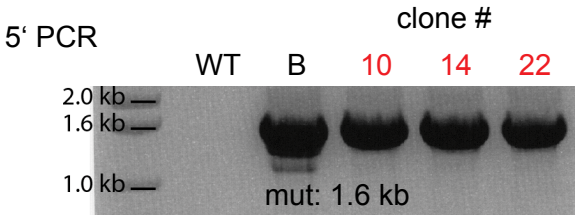

B: Positive control with targeted BAC
V: Negative control with targeting vector
WT: Negative control with wild-type genomic DNA

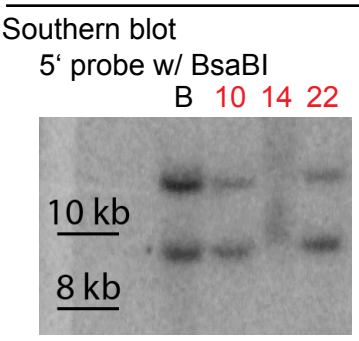

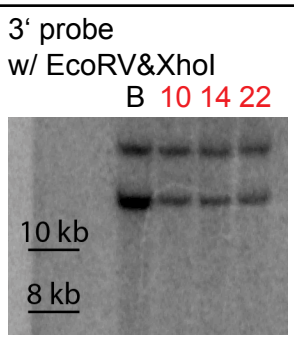

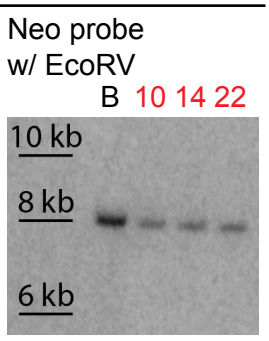

Jang264150_Fig. S3

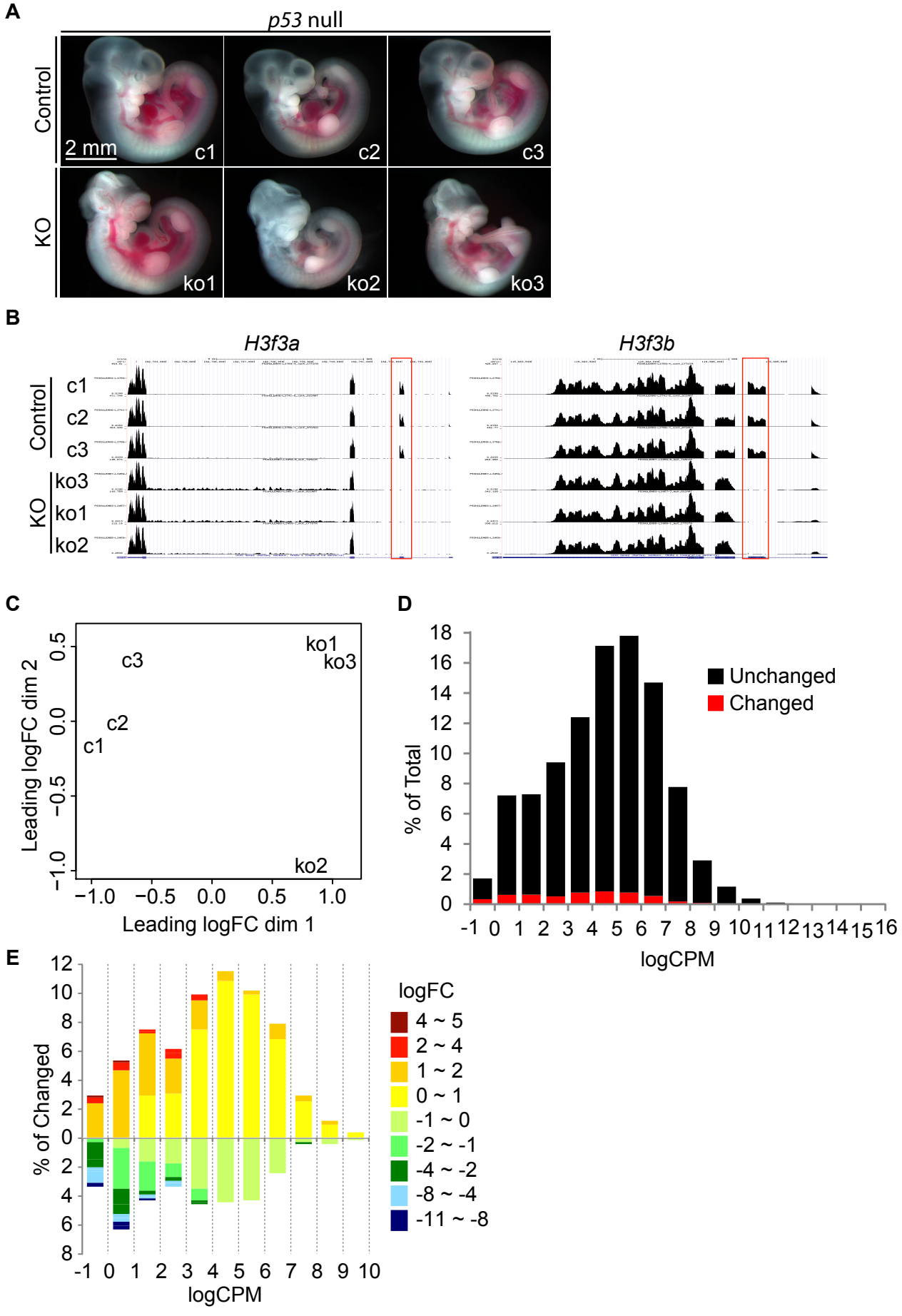

Jang264150_Fig. S3

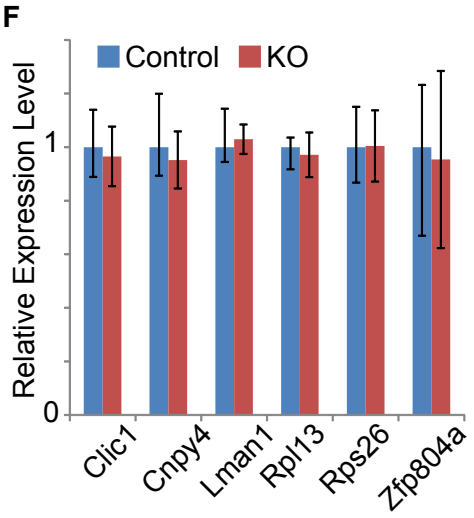

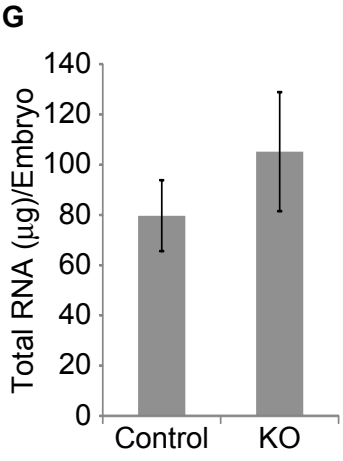

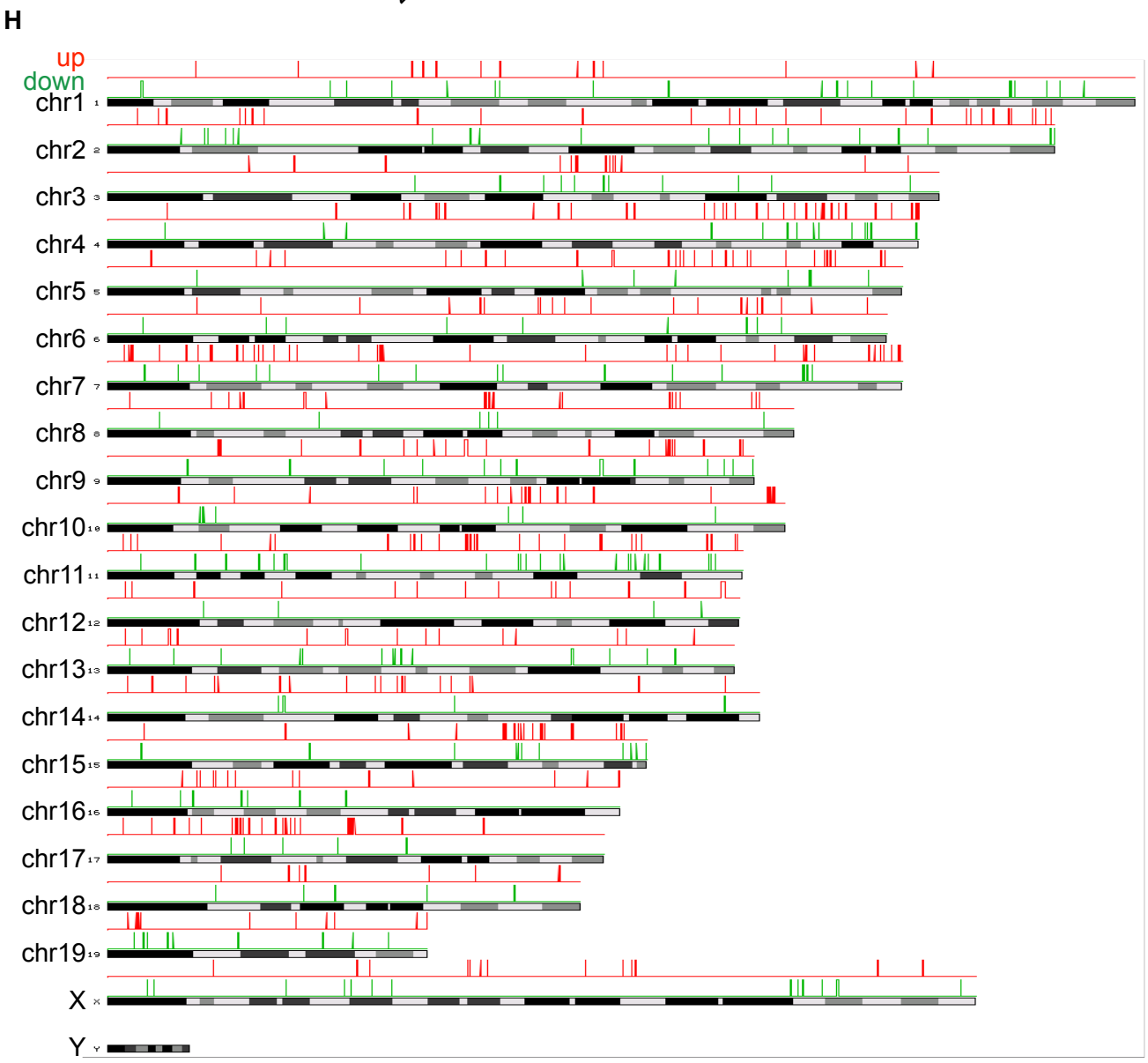

Jang264150_Fig. S3

I

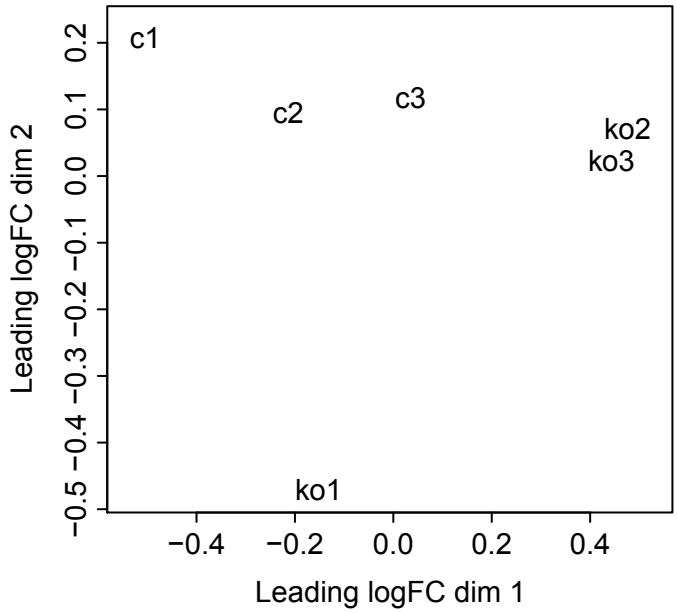

J

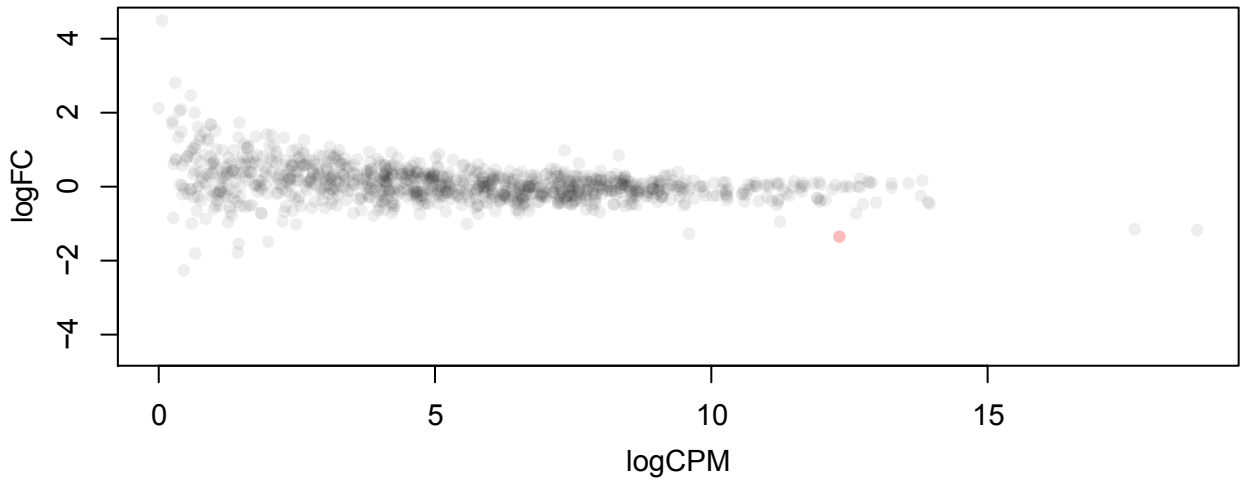

Jang264150_Fig. S4

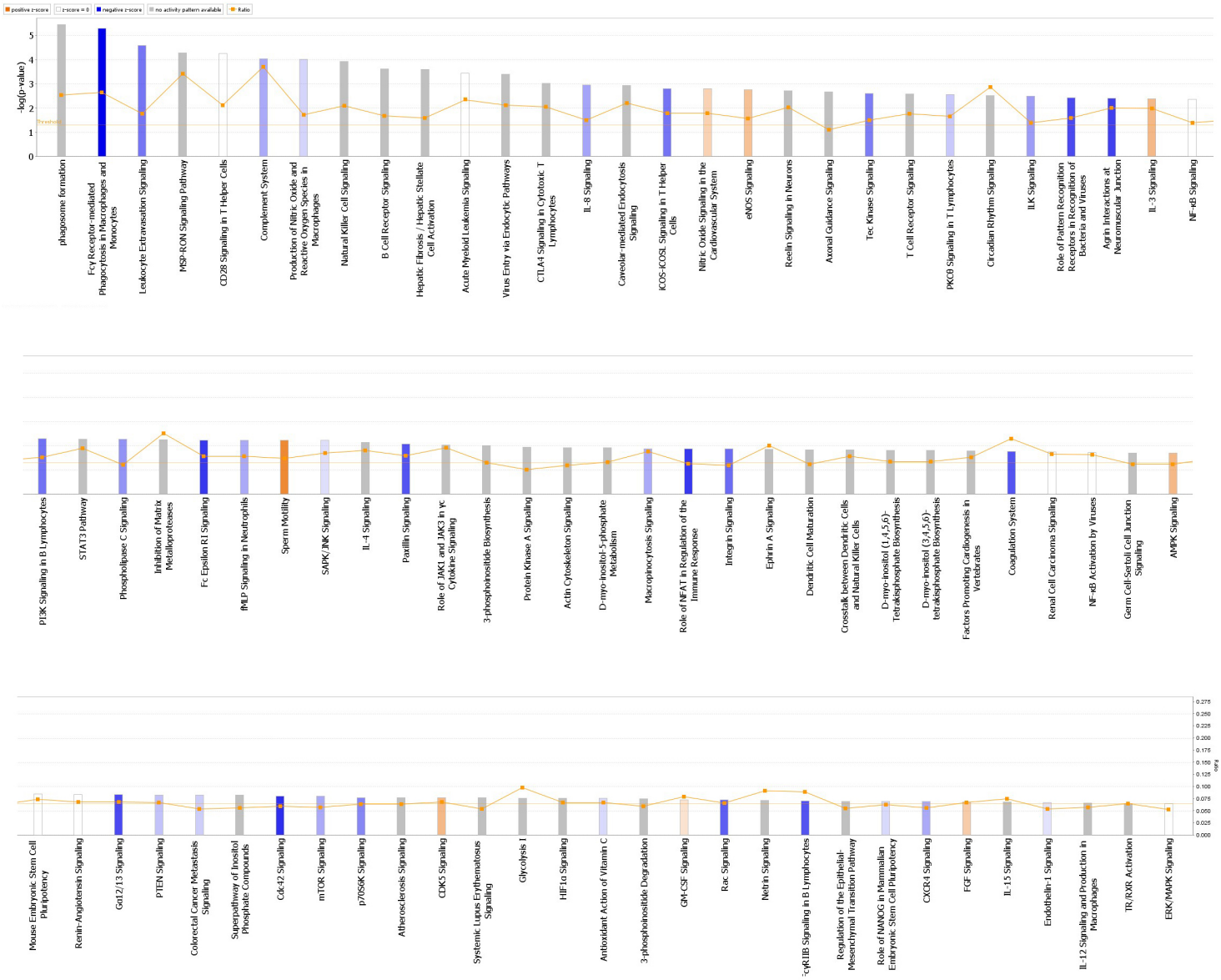

Jang264150_Fig. S5

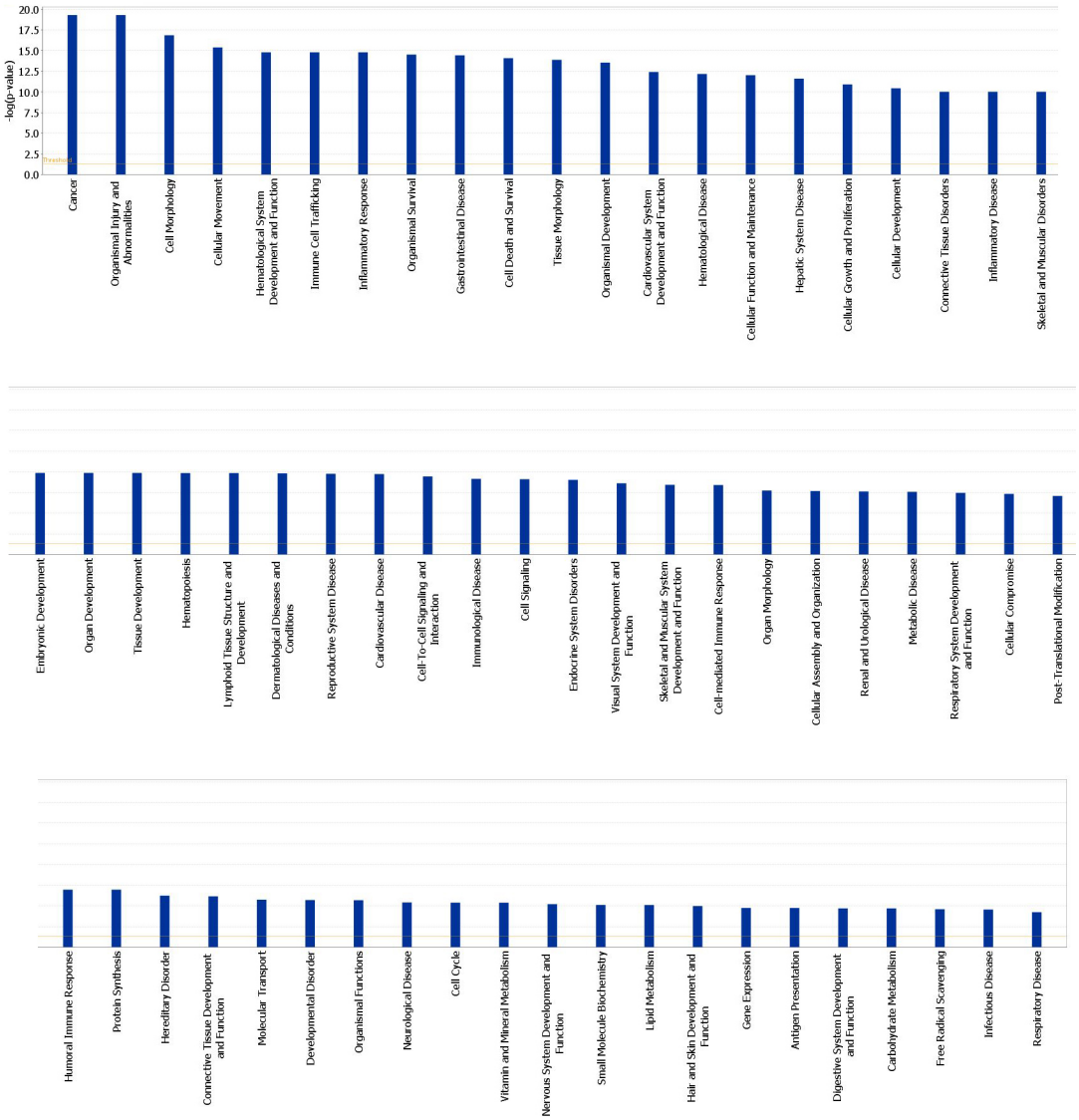

Jang264150_Fig. S6

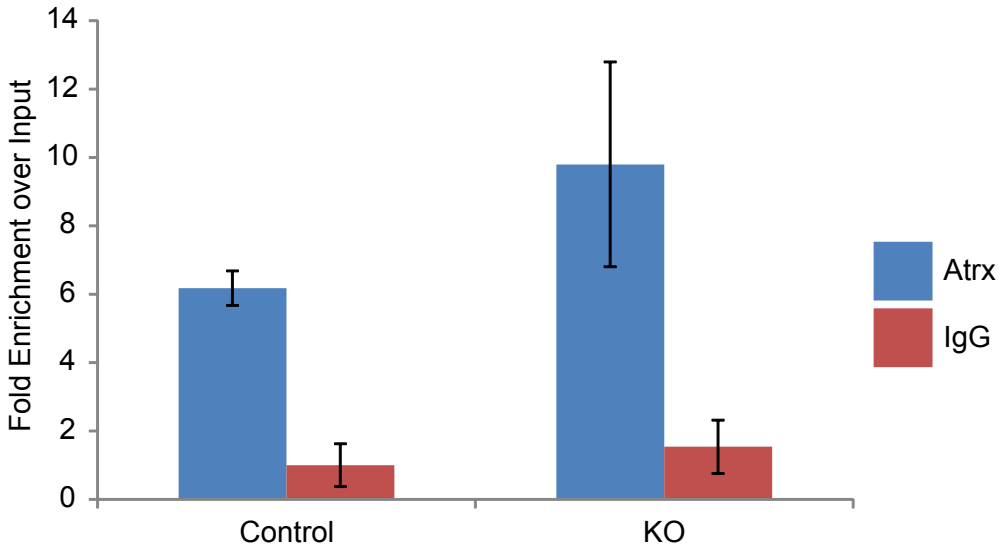

Jang264150_Fig. S7